

Measuring a Binary Black Hole Eccentrically Orbiting a Galactic Nucleus with Gravitational Waves: Interim Report 1

Andrew Laeuger

July 2022

1 Overview and Background

Since the first detection of gravitational waves (GWs) by LIGO in 2015, GW astronomy has cemented itself as a legitimate and advantageous method for observing binary systems of compact objects, the majority of which are binary black holes (BBHs) [10, 2, 1]. Currently, the ground detectors in LIGO/Virgo/KAGRA are most sensitive between 10 Hz to a few kHz, which describes the final moments before merger. In order for a GW detector to be sensitive to frequencies below 1 Hz, it must be built in space, where forming an interferometer with arm lengths much greater than LIGO's is feasible. LISA is a planned space based detector which would specialize in the millihertz band $\sim 10^{-3} - 10^{-1}$ Hz [12].

There are detector concepts which lie in the decihertz range – between LISA and ground-based detectors – such as B-DECIGO [7] and TianGO [8, 9], which may expand the range of astrophysical systems we can observe via GWs. These space-borne GW observatories could monitor inspiraling compact binary systems at times long before their orbital frequencies climb into the frequency bands of active ground-based detectors. Furthermore, since the instantaneous orbital decay timescale due to GW emission varies as $\tau_{GW} \propto f_{orb}^{-8/3}$ [11], a stellar-mass BBH system will remain in the frequency band of these low-frequency observatories much longer than in the frequency band of ground-based experiments. This will allow space-based observatories to monitor properties of a BBH system which may change over time scales on the order of years.

Consider a system consisting of a BBH orbiting around a nearby supermassive black hole (SMBH), which is sketched out in Fig. 1 along with the relative orientation of a hypothetical space-based GW observatory. When a BBH is in such a hierarchical triple system with the SMBH, the orbit of the BBH's center of mass about the SMBH (called the "outer orbit") produces a Doppler shift of the GW frequency [4]. Furthermore, when the semimajor axis of the outer orbit a_o is small enough, the angular momentum of the inner orbit (the BBH), \mathbf{L}_i , will precess about the angular momentum of the outer orbit, \mathbf{L}_o . This coupling between the orbit of the BBH around the SMBH and the inner angular momentum is called de Sitter precession. The inner orbit angular momentum \mathbf{L}_i evolves under de Sitter precession as

$$\frac{d\hat{\mathbf{L}}_i}{dt} = \Omega_{dS} \hat{\mathbf{L}}_o \times \hat{\mathbf{L}}_i \quad (1)$$

where

$$\Omega_{dS} = \Omega_0 \frac{M_3}{a_o(1 - e_o^2)} \quad (2)$$

and $\Omega_0 = \sqrt{M_3/a_o^3}$ ¹. For GWs emitted from the BBH with sufficiently low frequency, these perturbations due to the SMBH can be inferred from the waveform. Recently, Hang Yu and Yanbei Chen, with whom I will be working with this summer, studied how observations of the dS precession and Doppler shift in a hierarchical triple can allow inference of the mass of the SMBH, M_3 , the semimajor axis of the outer orbit, a_o , and the eccentricity of the outer orbit, e_o , through the modulation of the detected GW waveform [13]. In particular, they find that if the precession period P_{dS} is comparable to the duration of observation by a space-borne GW observatory, then the dS precession of \mathbf{L}_i can be detected and combined with Doppler shift measurements to generate estimates of the triple system parameters to percent-level precision.

¹We use geometric units in this paper where $G = c = 1$.

where

$$\left(\tilde{g}|\tilde{h}\right) = 4 \operatorname{Re} \int_0^\infty \frac{\tilde{g}^*(f)\tilde{h}(f)}{S_n(f)} df, \quad (4)$$

\tilde{h} is the frequency-domain waveform, $S_n(f)$ is the PSD of the detector noise, and θ_a and θ_b are the various parameters of the system:

θ^a	Definition
$\log \mathcal{M}_z$	Detector Frame Chirp Mass: $\mu^{3/5}(m_1 + m_2)^{2/5}$
q	Mass Ratio m_1/m_2
$\log D_L$	Luminosity Distance
t_c	Coalescence Time
ϕ_c	Coalescence Phase
$\bar{\theta}_S, \bar{\phi}_S$	Line of Sight of BBH+SMBH Triple
$\bar{\theta}_J, \bar{\phi}_J$	Orientation of Total Angular Momentum \mathbf{J}
λ_L	Angle Between \mathbf{L}_i and \mathbf{L}_o
α_0	Initial Phase of \mathbf{L}_i Around \mathbf{L}_o
$\log M_3$	SMBH Mass
$\log a_o$	Outer Orbit Semimajor Axis
$\phi^{(0)}$	Outer Orbit Initial Phase
e_o	Outer Orbit Eccentricity

Table 1: Relevant parameters in BBH+SMBH triple system for GW observed by detectors. Bars over angles indicate the Solar System coordinate frame.

For a network of GW detectors, the Fisher matrix is just the sum of the Fisher matrices from each detector on its own. The covariance matrix Σ_{ab} , which allows us to compute parameter uncertainties, is related to the Fisher matrix roughly as:

$$\Sigma_{ab} = [\Gamma^{-1}]_{ab} + \mathcal{O}(\rho^{-4}), \quad (5)$$

So as long as the SNR ρ is large, we can estimate the covariance matrix as the inverse of the Fisher matrix. The covariance matrix suggests that $(\Delta\theta_i)^2 = \Sigma_{ii}$, so in order to find the parameter estimation uncertainties, we need only examine the diagonal elements of the covariance matrix.

Ultimately, as long as one can describe the frequency-domain waveform for gravitational waves emitted from a BBH+SMBH triple, we can apply the Fisher matrix method to quantify the parameter estimation uncertainty. Enumerating such a waveform can be a difficult task, as this often requires forgoing an analytic solution for the equations of GR in favor of a post-Newtonian expansion. Fortunately, previous works have done so for some limiting cases, and some terms which contribute to the measured strain $\tilde{h}(f)$ are given in [13]. However, I will need to generalize these forms to account for non-zero eccentricities, which will also expand the size of the Fisher matrix by a few additional terms.

3 Current Progress

My work began by applying the Fisher information matrix method described above to a simple binary black hole system. In particular, I wrote code that placed three detectors on the surface of the Earth (namely, in the positions and orientations of Hanford, Livingston, and VIRGO) and calculated the strain measured in each detector from the gravitational waves emitted from a merging BBH. Then, using that code, I could calculate the derivative of the frequency-domain waveform with respect to its various relevant parameters, and thus systematically compute the Fisher matrix. After computing the inverse of the Fisher matrix, I could use the terms on the diagonal to estimate the uncertainty in parameter estimation by this three-detector network. This sequence allows for determination of the parameter estimation uncertainty for a given single set of BBH parameter values, so in order to understand how the estimation precision depends on those values, I needed to repeat this process over a range of possible values. For example, in Fig. 2 below, the

left-hand plot shows how the fractional error in the chirp mass \mathcal{M} depends on the luminosity distance to the BBH and the chirp mass itself.

It is perhaps counterintuitive that even though the strain increases in magnitude with increasing chirp mass ($|\tilde{h}(f)| \sim \mathcal{M}^{5/6}$), our ability to measure the chirp mass declines. However, this can be explained by recalling that the Fisher matrix scales with the derivative of the frequency-domain waveform, essentially reflecting how sensitive the strain is to changing parameters. For chirp masses on the scale of tens of solar masses, the contribution of the chirp mass to the GW phase is actually the strongest contribution, for:

$$\frac{d\tilde{h}}{d(\log \mathcal{M})} = \mathcal{M} \frac{d\tilde{h}}{d\mathcal{M}} = \frac{5}{6}\tilde{h} + C_1\mathcal{M}^{-5/3}\tilde{h} + C_2\mathcal{M}^{-1}\tilde{h} \sim \mathcal{M}^{-5/6} \quad (6)$$

So, examining rough dimensional dependencies, we can see that

$$\Gamma_{\log \mathcal{M} \log \mathcal{M}} \sim \left(\frac{d\tilde{h}}{d(\log \mathcal{M})} \right)^2 \sim \mathcal{M}^{-5/3} \rightarrow \Sigma_{\log \mathcal{M} \log \mathcal{M}} \sim \mathcal{M}^{5/3} \rightarrow \Delta(\log \mathcal{M}) \approx \frac{\Delta \mathcal{M}}{\mathcal{M}} \sim \mathcal{M}^{5/6} \quad (7)$$

thus predicting that increasing chirp mass corresponds to increasing fractional uncertainty in measuring that parameter. On the right side of Fig. 2, the fractional uncertainty in measuring D_L is depicted. Now, $\frac{d\tilde{h}}{d \log D_L} = -\tilde{h}$, so in this case, a stronger signal will correspond to better parameter estimation precision. Indeed, this is what we see in the contour plot: the strain decreases with increasing D_L , so the fractional uncertainty in D_L grows with increasing D_L , and the contribution from both GW polarizations is weakest when the BBH is viewed edge-on, so the uncertainty is greatest when the the angular momentum of the BBH is perpendicular to our line of sight.

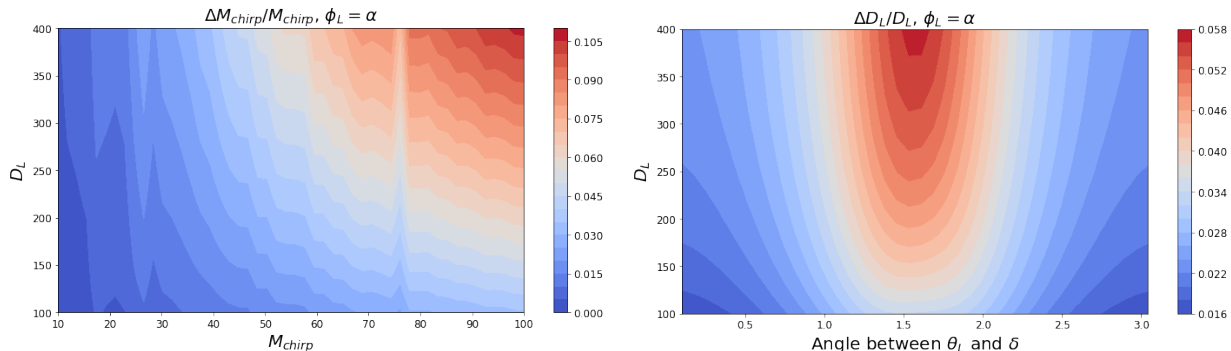


Figure 2: Left: Fractional error in \mathcal{M} measurable by network of three ground-based GW observatories for varying \mathcal{M} and D_L , assuming the azimuthal angles of the line of sight and angular momentum are equal. Right: Fractional error in D_L measurable by network of three ground-based GW observatories for varying $\theta_L - \delta$ and D_L , assuming the azimuthal angles of the line of sight and angular momentum are equal.

I have now moved onto studying triple systems (BBH+SMBH) with an L-shaped space-based detector, such as the proposed TianGO project. The geometry in this case is much more involved, as we must now account for the orientation of the BBH angular momentum relative to the outer orbit angular momentum as well as its precession due to the SMBH, in addition to all the parameters we needed to describe the BBH on its own. I am currently investigating whether Mathematica or Python are optimal for efficiently calculating the parameter estimation uncertainties both accurately and efficiently. I will then proceed to reproduce the results of [13], where the outer orbit of the BBH around the SMBH is circular, and after doing so, begin to implement changes to allow for eccentric outer orbits.

One unexpected difficulty I have faced in this work has been the limitations of computers in generating high-precision numbers. When computing the Fisher matrix, the various derivatives of \tilde{h} can result in elements differing from one another in by more than ten orders of magnitude. With a machine precision that is only limited to a finite number of bits per number, the contributions of small numbers in computations (inverting Γ , for example) can be washed out, leading to unrealistic results (i.e., negative values on the diagonal of the covariance matrix). Fixing these kinds of problems is unfortunately not something that can be done easily, since they are intrinsically tied to the properties of standard computing hardware. The best

solution I have implemented thus far is to exclude certain parameters from the Fisher matrix which the waveform is highly sensitive to. These parameters are manifest as large entries in the diagonals of the Fisher matrix, corresponding to low uncertainties. When studying parameters with much smaller contributions to the Fisher matrix, we can effectively say that the parameters with large Fisher matrix terms are known very well, and then exclude them from the calculation so that when inverting the new Fisher matrix, the terms do not span as many orders of magnitude.

4 Acknowledgments

I'd like to thank Brian Seymour and Yanbei Chen for their tremendous support in this project. I also gratefully acknowledge the support from the National Science Foundation Research Experience for Undergraduates (NSF REU) program, the California Institute of Technology, and the LIGO Summer Undergraduate Research Fellowship.

References

- [1] B. P. Abbott et al. Observation of Gravitational Waves from a Binary Black Hole Merger. *Phys. Rev. Lett.*, 116(6):061102, 2016.
- [2] R. Abbott et al. GWTC-2: Compact Binary Coalescences Observed by LIGO and Virgo During the First Half of the Third Observing Run. *Phys. Rev. X*, 11:021053, 2021.
- [3] B.M. Peterson. Measuring the Masses of Supermassive Black Holes. *Space Sci. Rev.*, 183(253), 2014.
- [4] Curt Cutler. Angular resolution of the LISA gravitational wave detector. *Phys. Rev. D*, 57:7089–7102, 1998.
- [5] Curt Cutler and Eanna E. Flanagan. Gravitational waves from merging compact binaries: How accurately can one extract the binary’s parameters from the inspiral wave form? *Phys. Rev. D*, 49:2658–2697, 1994.
- [6] H. Yu, Y. Wang, B. Seymour, and Y. Chen. Detecting gravitational lensing in hierarchical triples in galactic nuclei with space-borne gravitational-wave observatories. *arXiv e-prints*, 2021. arXiv:2107.14318.
- [7] Seiji Kawamura et al. Current status of space gravitational wave antenna DECIGO and BDECIGO, 6 2020.
- [8] Kevin A. Kuns. *Future Networks of Gravitational Wave Detectors: Quantum Noise and Space Detectors*. PhD thesis, University of California, Santa Barbara, 3 2019.
- [9] Kevin A. Kuns, Hang Yu, Yanbei Chen, and Rana X. Adhikari. Astrophysics and cosmology with a decihertz gravitational-wave detector: TianGO. *Phys. Rev. D*, 102(4):043001, 2020.
- [10] LIGO Scientific Collaboration and Virgo Collaboration. GWTC-1: A Gravitational-Wave Transient Catalog of Compact Binary Mergers Observed by LIGO and Virgo during the First and Second Observing Runs. *Physical Review X*, 9(031040), 2019. arXiv:1811.12907.
- [11] Michele Maggiore. *Gravitational Waves. Vol. 1: Theory and Experiments*. Oxford Master Series in Physics. Oxford University Press, 2007.
- [12] P. Amaro-Seoane, H. Audley, S. Babak, J. Baker, E. Barausse, P. Bender, E. Berti, P. Binetruy, et al. Laser Interferometer Space Antenna. *arXiv e-prints*, 2017. arXiv:1702.00786.
- [13] Hang Yu and Yanbei Chen. Direct determination of supermassive black hole properties with gravitational-wave radiation from surrounding stellar-mass black hole binaries. *Phys. Rev. Lett.*, 126(2):021101, 2021.